2

Autophagy-Mediated Defense Response of Mouse Mesenchymal Stromal Cells (MSCs) to Challenge with *Escherichia coli*

N.V. Gorbunov[1,*], B.R. Garrison[1], M. Zhai[1], D.P. McDaniel[2], G.D. Ledney[3], T.B. Elliott[3] and J.G. Kiang[3,*]

[1]*The Henry M. Jackson Foundation for the Advancement of Military Medicine, Inc.*
[2]*The Department of Microbiology and Immunology, School of Medicine,*
[3]*Radiation Combined Injury Program, Armed Forces Radiobiology Research Institute, Uniformed Services University of the Health Sciences, Bethesda, Maryland, USA*

1. Introduction

Symbiotic microorganisms are spatially separated from their animal host, e.g., in the intestine and skin, in a manner enabling nutrient metabolism as well as evolutionary development of protective physiologic features in the host such as innate and adaptive immunity, immune tolerance, and function of tissue barriers (1,2). The major interface barrier between the microbiota and host tissue is constituted by epithelium, reticuloendothelial tissue, and mucosa-associated lymphoid tissue (MALT) (2,3).

Traumatic damage to skin and the internal epithelium in soft tissues can cause infections that account for 7% to 10% of hospitalizations in the United States (4). Moreover, wound infections and sepsis are an increasing cause of death in severely ill patients, especially those with immunosupression due to exposure to cytotoxic agents and chronic inflammation (4). It is well accepted that breakdown of the host-bacterial symbiotic homeostasis and associated infections are the major consequences of impairment of the "first line" of anti-microbial defense barriers such as the mucosal layers, MALT and reticuloendothelium (1-3). Under these impairment conditions of particular interest then is the role of sub-mucosal structures, such as connective tissue stroma, in the innate defense compensatory responses to infections.

The mesenchymal connective tissue of different origins is a major source of multipotent mesenchymal stromal cells (i.e., colony-forming-unit fibroblasts) (5, 6). Recent discovery of immunomodulatory function of mesenchymal stromal cells (MSCs) suggests that they are essential constituents that control inflammatory responses (6-7).

Recent *in vivo* experiments demonstrate promising results of MSC transfusion for treatment of acute sepsis and penetrating wounds (7-9). The molecular mechanisms underlying MSC

* Corresponding Authors

Report Documentation Page

Form Approved
OMB No. 0704-0188

1. REPORT DATE	2. REPORT TYPE	3. DATES COVERED
MAR 2012		**00-00-2012 to 00-00-2012**

4. TITLE AND SUBTITLE	5a. CONTRACT NUMBER
Autophagy-Mediated Defense Response Of Mouse Mesenchymal Stromal Cells (MSCs) To Challenge With Escherichia Coli	5b. GRANT NUMBER
	5c. PROGRAM ELEMENT NUMBER
6. AUTHOR(S)	5d. PROJECT NUMBER
	5e. TASK NUMBER
	5f. WORK UNIT NUMBER
7. PERFORMING ORGANIZATION NAME(S) AND ADDRESS(ES) **Uniformed Services University of the Health Sciences,Radiation Combined Injury Program,Bethesda,MD,20814**	8. PERFORMING ORGANIZATION REPORT NUMBER
9. SPONSORING/MONITORING AGENCY NAME(S) AND ADDRESS(ES)	10. SPONSOR/MONITOR'S ACRONYM(S)
	11. SPONSOR/MONITOR'S REPORT NUMBER(S)

12. DISTRIBUTION/AVAILABILITY STATEMENT
Approved for public release; distribution unlimited

13. SUPPLEMENTARY NOTES
1/20, Book Chapter in Protein Interactions March, 2012

14. ABSTRACT
Symbiotic microorganisms are spatially separated from their animal host, e.g., in the intestine and skin, in a manner enabling nutrient metabolism as well as evolutionary development of protective physiologic features in the host such as innate and adaptive immunity, immune tolerance, and function of tissue barriers (1,2). The major interface barrier between the microbiota and host tissue is constituted by epithelium reticuloendothelial tissue, and mucosa-associated lymphoid tissue (MALT) (2,3).

15. SUBJECT TERMS

16. SECURITY CLASSIFICATION OF:			17. LIMITATION OF ABSTRACT	18. NUMBER OF PAGES	19a. NAME OF RESPONSIBLE PERSON
a. REPORT	b. ABSTRACT	c. THIS PAGE			
unclassified	**unclassified**	**unclassified**	**Same as Report (SAR)**	**23**	

action in septic conditions are currently under investigation. It is known to date that (i) Gram-negative bacteria can induce an inflammatory response in MSCs *via* cascades of Toll-like receptor (type 4) and the nucleotide-binding oligomerization domain-containing protein 2 (NOD2) complexes recognizing the conserved pathogen-associated molecular patterns; (ii) activated MSCs can modulate the septic response of resident myeloid cells; and (iii) activated MSCs can directly suppress bacterial proliferation by releasing antimicrobial factors (10, 11).

Considering all of the above factors including the fact that MSCs are ubiquitously present in the sub-mucosal structures and conjunctive tissue, one would expect involvement of these cells in formation of antibacterial barriers and host-microbiota homeostasis. From this perspective our attention was attracted by the phagocytic properties of mesenchymal fibroblastic stromal cells documented in an early period of their investigation (5, 12). The phagocytosis mechanism is closely and synchronously connected with the cellular mechanisms of biodegradation mediated by the macroautophagy-lysosomal (autolysosomal) system (13-15). The last one decomposes proteins and organelles as well as bacteria and viruses inside cells and, therefore, is considered as a part of the innate defense mechanism (13- 15).

Macroautophagy (hereafter referred to as autophagy) is a catabolic process of bulk lysosomal degradation of cell constituents and phagocytized particles (16). Autophagy dynamics in mammalian cells are well described in recent reviews (14, 17-20). Thus, it was proposed that autophagy is initiated by the formation of the phagophore, followed by a series of steps, including the elongation and expansion of the phagophore, closure and completion of a double-membrane autophagosome (which surrounds a portion of the cytoplasm), autophagosome maturation through docking and fusion with an endosome (the product of fusion is defined as an amphisome) and/or lysosome (the product of fusion is defined as an autolysosome), breakdown and degradation of the autophagosome inner membrane and cargo through acid hydrolases inside the autolysosome, and recycling of the resulting macromolecules through permeases (14). These processes, along with the drastic membrane traffic, are mediated by factors known as autophagy-related proteins (i.e., ATG-proteins) and the lysosome-associated membrane proteins (LAMPs) that are conserved in evolution (21). The autophagic pathway is complex. To date there are over 30 ATG genes identified in mammalian cells as regulators of various steps of autophagy, e.g., cargo recognition, autophagosome formation, etc. (14, 22). The core molecular machinery is comprised of (i) components of signaling cascades, such as the ULK1 and ULK2 complexes and class III PtdIns3K complexes, (ii) autophagy membrane processing components, such as mammalian Atg9 (mAtg9) that contributes to the delivery of membrane to the autophagosome as it forms, and two conjugation systems: the microtubule-associated protein 1 (MAP1) light chain 3 (i.e., LC3) and the Atg12–Atg5–Atg16L complex. The two conjugation systems are proposed to function during elongation and expansion of the phagophore membrane (14, 19, 22, 23). A conservative estimate of the autophagy network counts over 400 proteins, which, besides the ATG-proteins, also include stress-response factors, cargo adaptors, and chaperones such as p62/SQSTM1 and heat shock protein 70 (HSP70) (15, 19, 22, 24, 26-28).

Autophagy is considered as a cytoprotective process leading to tissue remodeling, recovery, and rejuvenation. However, under circumstances leading to mis-regulation of the

autolysosomal pathway, autophagy can eventually cause cell death, either as a precursor of apoptosis in apoptosis-sensitive cells or as a result of destructive self-digestion (29).

Based on this information we hypothesized that challenge of MSCs with *Escherichia coli* (*E. coli*) can induce a complex process where bacterial phagocytosis is accompanied by activation of autolysosomal pathway and stress-adaptive responses in MSCs. The objective of this current chapter is to provide evidence of this hypothesis.

2. Hypothesis test: Experimental procedures and technical approach

2.1 Bone marrow stromal cells

Bone marrow stromal cells were obtained from 3- to 4-month-old B6D2F1/J female mice using a protocol adapted from STEMCELL Technologies, Inc., and were expanded and cultivated in hypoxic conditions (5% O_2, 10% CO_2, 85% N_2) for approximately 30 days in MESENCULT medium (STEMCELL Technologies, Inc.) in the presence of antibiotics. Phenotype, proliferative activity, and colony-forming ability of the cells were analyzed by flow cytometry and immunofluorescence imaging using positive markers for mesenchymal stromal cells: CD44, CD105, and Sca1. The results of these analyses showed that the cultivated cells displayed properties of mesenchymal stromal clonogenic fibroblasts.

The experiments were performed in a facility accredited by the Association for the Assessment and Accreditation of Laboratory Animal Care-International (AAALAC-I). All animals used in this study received humane care in compliance with the Animal Welfare Act and other federal statutes and regulations relating to animals and experiments involving animals and adhered to principles stated in the Guide for the Care and Use of Laboratory Animals, NRC Publication, 1996 edition.

2.2 Challenge of MSCs with *Escherichia coli* bacteria

MSC cultures of approximate 80% confluency were challenged with proliferating *E. coli* ($1x10^7$ microorganisms/ml) for 1-5 h in antibiotic-free media. For assessment of the cellular alteration ≥ 5 h the incubation medium was replaced with fresh medium containing penicillin and streptavidin antibiotics. Bacteria-cell interaction was monitored with time-lapse microscopy using DIC imaging of MSCs and fluorescence imaging of *E. coli* labeled with PSVue® 480, a fluorescent cell tracking reagent (www.mtarget.com). At the end of the experiments the cells were either (i) harvested, washed, and lysed for qRT-PCR and immunoblot analyses, (ii) fixed for transmission electron microscopy and fluorescence confocal imaging, or (iii) used live for imaging of Annexin V reactivity, dihydrorhodamine 123, a sensitive indicator of peroxynitrite reactivity, and colony formation. With this protocol the cells were tested for (i) phagocytic activity; (ii) autolysosomal activity; (iii) production of reactive oxygen (ROS) and nitrogen species, (iii) stress responses to *E. coli*; (iv) genomic DNA damage and pro-apoptotic alterations; and (v) colony-forming ability. The results of observations indicated that challenge with *E. coli* did not diminish viability and colony forming ability of the cells under the selected conditions (Fig.1). Stimulation of MSCs with *E. coli* resulted in expression of the proinflammatory genes, IL-1α, IL-1β, IL-6, and iNOS, as determined with qRT-PCR analysis.

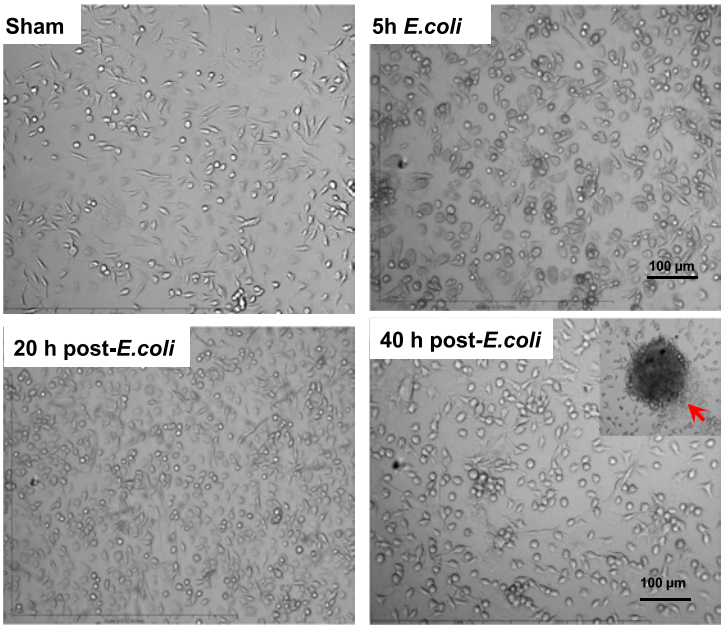

Conditions: MSCs were incubated with ~1x10^7/ml *E. coli* for 5 h in medium (without antibiotics). After 5 h the medium was replaced with fresh medium (with antibiotics) and MSCs were incubated for another 40 h. Inset: formation of colonies (red arrowhead) occurred at 72 h post-exposure to *E. coli.*

Fig. 1. Bright field microscopy of MSCs challenged with *E. coli*. Images presented in the panels are MSCs at different time-points following exposure of MSCs to *E. coli*.

2.3 Analysis of the cell proteins

Proteins from MSCs were extracted in accordance with the protocol described previously (30). The aliquoted proteins (20 µg total protein per gel well) were separated on SDS-polyacrylamide slab gels (NuPAGE 4-12% Bis-Tris; Invitrogen, Carlsbad, CA). After electrophoresis, proteins were blotted onto a PDVF membrane and the blots were incubated with antibodies (1 µg/ml) raised against MAP LC3, Lamp-1, p62/SQSTM1, p65(NFκB), Nrf2, HSP70, iNOS, and actin (Abcam, Santa Cruz Biotechnology Inc., LifeSpan Biosciences, Inc., eBiosciences) followed by incubation with species-specific IgG peroxidase conjugate. IgG amounts did not alter after radiation. IgG, therefore, was used as a control for protein loading.

2.4 Immunofluorescent staining and image analysis

MSCs (5 specimens per group) were fixed in 2% paraformaldehyde and analyzed with fluorescence confocal microscopy following labeling (30). Normal donkey serum and antibody were diluted in phosphate-buffered saline (PBS) containing 0.5% BSA and 0.15% glycine. Any nonspecific binding was blocked by incubating the samples with purified normal donkey serum (Santa Cruz Biotechnology, Inc., Santa Cruz, CA) diluted 1:20. Primary antibodies were raised against MAP LC3, Lamp-1, p62/SQSTM1, p65(NFκB),

Nrf2, Tom 20, and iNOS. That was followed by incubation with secondary fluorochrome-conjugated antibody and/or streptavidin-AlexaFluor 610 conjugate (Molecular Probes, Inc., Eugene OR), and with Hoechst 33342 (Molecular Probes, Inc., Eugene OR) diluted 1:3000. Secondary antibodies used were AlexaFluor 488 and AlexaFluor 594 conjugated donkey IgG (Molecular Probes Inc., Eugene OR). Negative controls for nonspecific binding included normal goat serum without primary antibody or with secondary antibody alone. Five confocal fluorescence and DIC images of crypts (per specimen) were captured with a Zeiss LSM 7100 confocal microscope. The immunofluorescence image analysis was conducted as described previously (30).

2.5 Transmission Electron Microscopy (TEM)

MSCs in cultures were fixed in 4% formaldehyde and 4% glutaraldehyde in PBS overnight, post-fixed in 2% osmium tetroxide in PBS, dehydrated in a graduated series of ethanol solutions, and embedded in Spurr's epoxy resin. Blocks were processed as described previously (30). The sections of embedded specimens were analyzed with a Philips CM100 electron microscope.

2.6 RNA isolation and qRT-PCR

Total cellular RNA was isolated from MSC pellets using the Qiagen RNeasy miniprep kit, quantified by measuring the absorbance at 260nm on a Nanodrop, and qualified by electrophoresis on a 1.2% agarose gel. cDNA was synthesized using Superscript II (Invitrogen) and qRT-PCR was performed using SYBR Green iQ Supermix (Bio-Rad), each according to the manufacturers' instructions. The quality of qRT-PCR data were verified by melt curve analysis, efficiency determination, agarose gel electrophoresis, and sequencing. Relative gene expression was calculated by the method of Pfaffl using the formula $2^{-\Delta\Delta Ct}$(31).

2.7 Statistical analysis

Statistical significance was determined using one-way ANOVA followed by post-hoc analysis with pair-wise comparison by Tukey-Kramer test. Significance is reported at a level of $p<0.05$.

3. Response of MSCs to challenge with *E. coli*

3.1 Phagocytosis and autolysosomal degradation of *E. coli* bacteria by MSCs

TEM images presented in Fig. 2 show different stages of cell-bacterium interaction. The uptake of microorganisms occurred in at least two independent events. The first event encompassed engulfing and taking in particles by the cell membrane extrusions (Fig. 2A1). The second event was tethering and "zipping" of adhered particles by the cell plasma membrane (Fig. 2A2 – 2A5). The time–lapse fluorescence microscopy observation indicated that these events proceeded quickly and the uptake process required a few minutes (not shown). Thereafter, a significant amount of bacteria in MSCs was observed within 1 h of co-incubation of the cells. The phagocytized bacteria were subjected to autolysosomal

degradation (Fig 2B). Formation of the double-membrane autophagosomes, which incorporated bacteria, was observable in MSCs at 3 h of co-incubation and during a further period of observation. Fusion of autophagosomes with lysosomes also occurred at this period. Fragmentation of bacterial constituents was observed at 5 h of co-incubation and appearance of bacterial "ghosts" at 24 h (Fig. 2B).

Various cells eliminate bacterial microorganisms by autophagy, and this elimination is in many cases crucial for host resistance to bacterial translocation. Although autophagy is a non-selective degradation process, autophagosomes do not form randomly in the cytoplasm, but rather sequester the bacteria selectively (32, 33). Therefore, autophagosomes that engulf microbes are sometimes much larger than those formed during degradation of cellular organelles, suggesting that the elongation step of the autophagosome membrane is involved in bacteria-surrounding autophagy (33). The mechanism underlying selective induction of autophagy at the site of microbe phagocytosis remains unknown. However, it is likely mediated by pattern recognition receptors, stress-response elements, and adaptor proteins, e.g., p62/SQSTM1, which target bacteria and ultimately recruit factors essential for formation of autophagosomes (13,14, 33, 34).

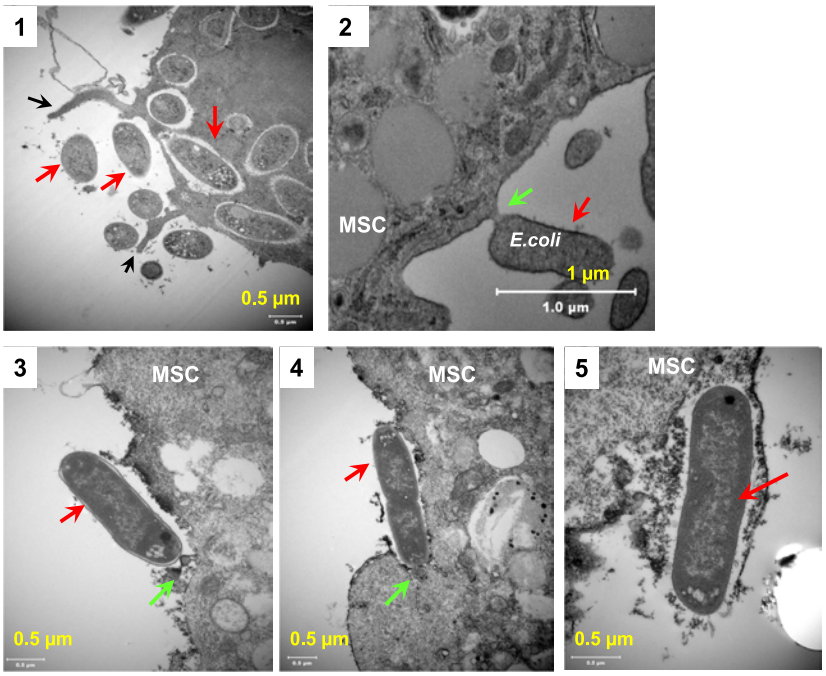

A

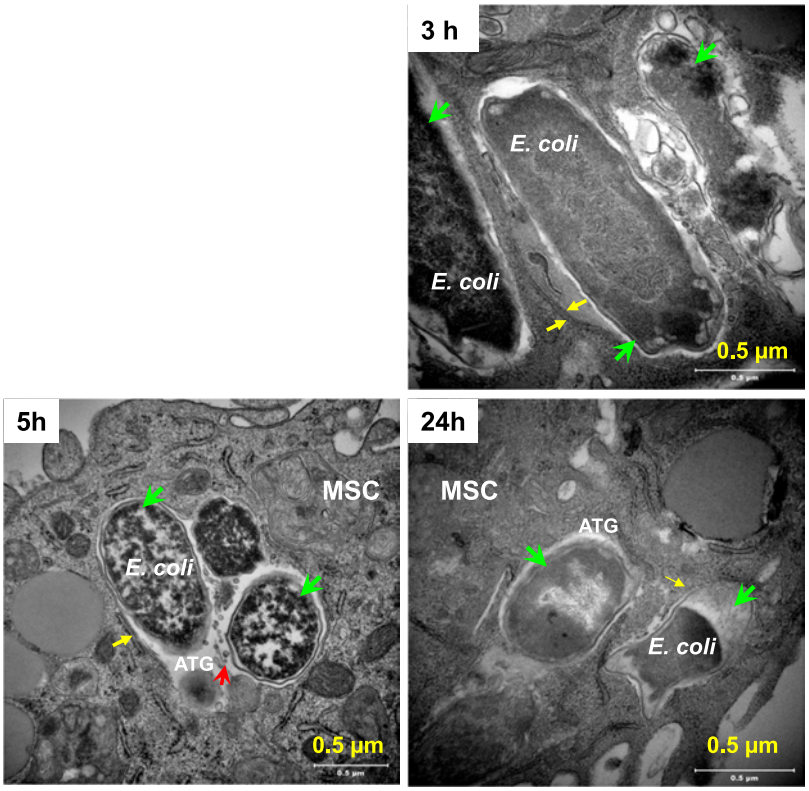

B

Conditions: MSCs were incubated with ~1x10^7/ml *E. coli* either for 3 h or 5 h in MesenCult Medium (without antibiotics). After 5 h the medium was replaced with fresh medium (with antibiotics) and MSCs were incubated for another 19 h.

Fig. 2. Transmission electron micrographs (TEM) of *E. coli* phagocytosis by MSCs and autolysosomal degradation of phagocytized bacteria.
A) Panel A1: Engulfing and up-take of bacteria (red arrows) by the cell plasma membrane extrusions (black arrows). Panels A2-A5: Tethering and zipping (green arrows) and up-take of bacteria (red arrows) by the cell plasma membrane. Specimens were fixed at 3 h co-incubation of MSCs with bacteria.
B) Autolysosomal degradation of phagocytized bacteria at different time-points after exposure of MSCs to *E. coli* (green arrows). Autophagosome (ATG) membranes are indicated with yellow arrows. Lysosome fusion with autophagosomes is indicated with red arrows.

The results of TEM were corroborated by the data obtained with immunoblotting and immunofluorescence confocal imaging of autophagy MAP (LC3) protein, lysosomal LAMP1 and the ubiquitin-associated target adaptor p62. A key step in the autophagosome biogenesis is the conversion of light-chain protein 3 type I (LC3-I, also known as ubiqitin-like protein, Atg8) to type II (LC3-II). The conversion occurs via the cleavage of the LC3-I carboxyl terminus by a redox-sensitive Atg4 cysteine protease. The subsequent binding of

the modified LC3-I to phosphatidylethanolamine, i.e., process of lipidation of LC3-I, on the isolation membrane, as it forms, is mediated by E-1- and E-2-like enzymes Atg7 and Atg3 (14). Therefore, conversion of LC3-I to LC3-II and formation of LC3-positive vesicles are considered to be a marker of activation of autophagy (14). A growing body of evidence suggests involvement of chaperone HSP70 in regulation of LC3-translocation. The results of immunoblot analysis of the proteins indicated an increase in the LC3-I to LC3-II – transition in the *E. coli* –challenged MSCs (Fig. 3).

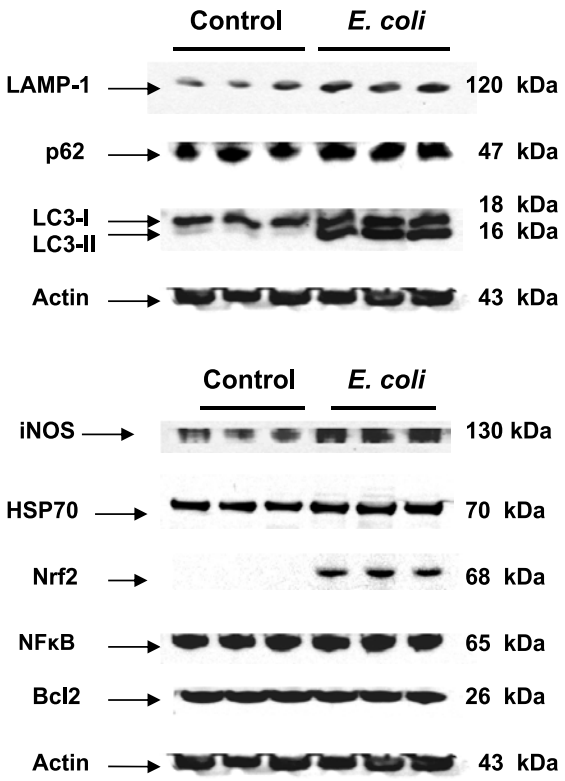

Conditions: MSCs were incubated with ~1x10^7/ml *E. coli* for 3 h in MesenCult Medium (without antibiotics). After 3 h the medium was replaced with fresh medium (with antibiotics) and MSCs were further incubated for another 21 h.

Fig. 3. Immunoblotting analysis of LC3, LAMP1 autolysosomal proteins, p62 adaptor protein, and stress-response elements: NF-κB(p65), Nrf2, HSP70 in MSCs challenged with *E. coli.*

The images presented in Fig. 4A indicate an increase of formation of LC3-positive vesicles in MSCs challenged with *E. coli*. The LC3 immunoreactivity co-localized with immunoreactivity to LAMP1, a marker of lysosomes, indicating presence of fusion of autophagosomes with lysosomes, i.e., formation of autolysosomes (Fig. 4A). This effect

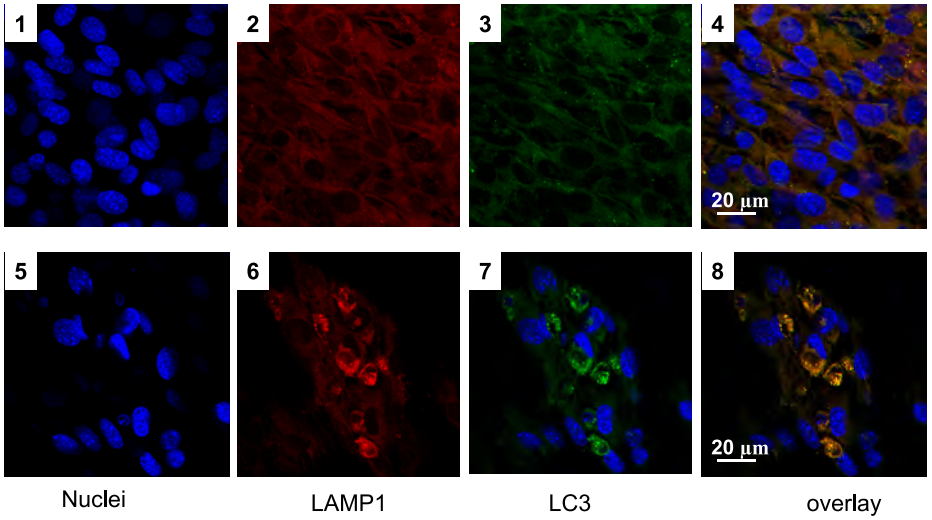

A

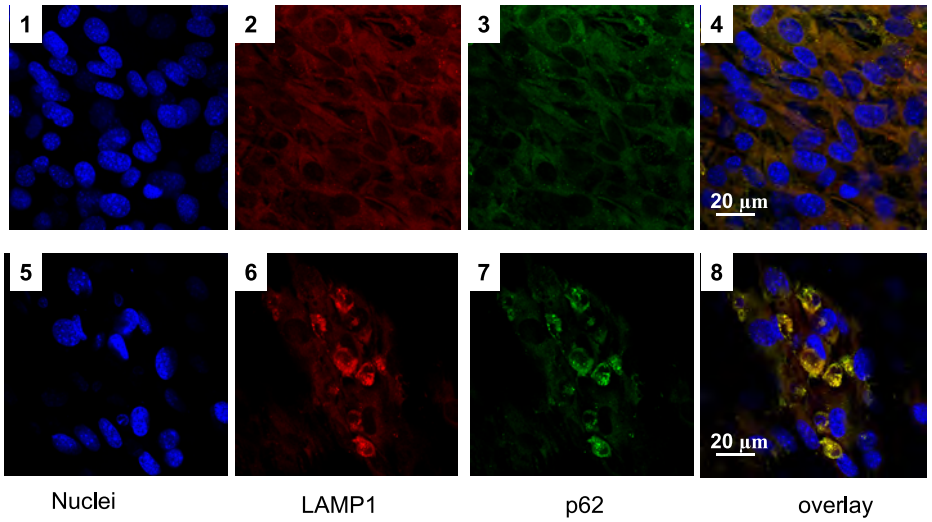

B

Conditions: MSCs were incubated with ~1x10^7 /ml *E. coli* for 3 h in MesenCult Medium (without antibiotics). After 3 h the medium was replaced with fresh medium (with antibiotics) and MSCs were further incubated for 21 h. Projections of LAMP1 protein (red channel) are shown in panels A2, A6, B2, and B6. Projections of LC3 protein (green channel) are shown in panels A3 and A7. Projections of p62 protein (green channel) are shown in panels B3 and B7. Counterstaining of nuclei was with Hoechst 33342 (blue channel). Panels A4, A8, B4, and B8 are overlay of signals acquired in the red, green, and blue channels. The confocal images were taken with pinhole setup to obtain 0.5 µm Z-sections.

Fig. 4. Immunofluorescence confocal imaging of the LC3, LAMP1, and p62 protein in MSCs challenged with *E. coli*. Panels A1-A4 and B1-B4 are control specimens. Panels A5-A8 and B5-B8 are challenged with *E. coli*.

was accompanied by the presence of immunoreactivity to p62, a marker of ubiquitin-dependent target transport, in autolysosomes that was associated with autophagy of *E. coli* (Fig. 4B, Fig. 5). The image analysis of autophagy was supported by results of immunoblotting of the proteins (Fig. 3). It should be noted that pre-incubation of cell cultures with wortmannin, an autophagy inhibitor, resulted in apoptotic transformations and ultimately loss of confluency approximately 3 h after challenge with *E. coli* (not shown).

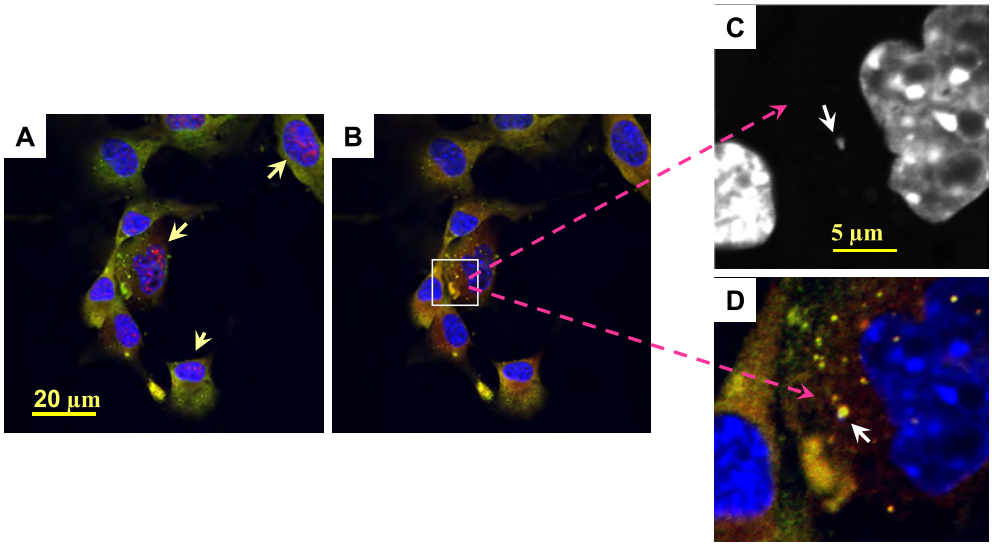

Panel A: Projection of FOXO3a (red channel; nuclear FOXO3a is indicated with yellow arrows) and p62 (green channel). Panel B: Projection of LC3 (red channel) and p62 (green channel). Counterstaining of nuclei with Hoechst 33342 appears in blue color. Panels C and D – selected area indicated in panel B.
Panel C: Signal acquired in the blue channel; bacterial DNA is indicated with white arrow.
Panel D: Signals acquired in the blue, red and green channels; co-localization of bacterial nucleus with p62 and LC3 proteins is indicated with white arrow.

Conditions: MSCs were incubated with ~1x10^7/ml *E. coli* for 3 h in MesenCult Medium (without antibiotics). After 3 h the medium was replaced with fresh medium (with antibiotics) and MSCs were incubated for further 21 h. The confocal images were taken with pinhole setup to obtain 0.5 µm Z-sections.

Fig. 5. Immunofluorescence confocal imaging of LC3, p62, phagocytized bacteria, and nuclear fraction of FOXO3a in MSCs challenged by *E. coli.*

Autolysosomal degradation of phagocytized bacteria can involve reactive oxygen and nitrogen species ultimately leading to up-regulation of stress-adaptive elements (13). Confocal fluorescence imaging of formation of reactive nitrogen species in autolysosomes was conducted using dihydrorhodamine 123, a sensitive indicator of peroxynitrite. The results of assessment of oxidative environment in the MSC autolysosomes containing *E. coli* are presented in Fig. 6. The appearance of reactivity to dihydrorhodamine 123 was likely

due to up-regulation of nitric oxide synthase induced in MSCs in response to challenge with *E. coli*. It was hypothesized this increase in redox events in MSCs could at least in part contribute to degradation of the phagocytized bacteria. Indeed, as shown in Fig. 7 bacterial nuclei present in autolysosomes were positive to terminal deoxynucleotidyl transferase dUTP nick-end labeling (TUNEL).

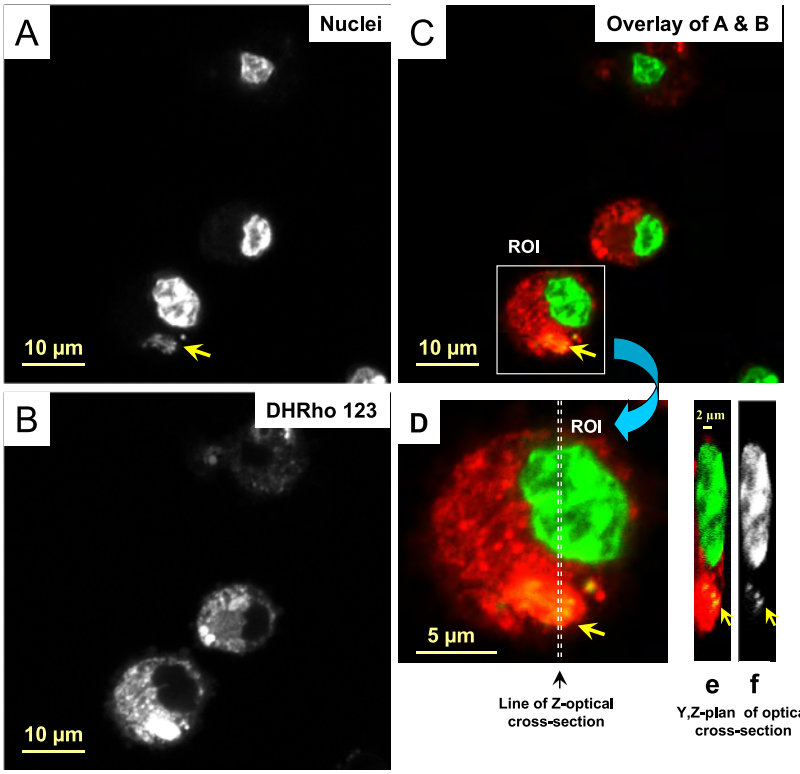

Panels A-C are projections of nuclei and oxidized fluorescent product of dihydrorhodamine 123. The images acquired in the blue (panel A) and green (panel B) are shown in grayscale; then, the images were overlaid in panel C in pseudo-colors that are "red" and "green", respectively. Panel D is the selected area indicated in panel C, where nuclei are green, oxidized dihydrorhodamine 123 (DHRho 123) is red, and co-localization of nuclei and DHRho 123 is in yellow colors. The presence of bacterial genomic DNA in the autolysosome appears in yellow as result of interference of red and green colors. Experimental conditions were the same as indicated in Fig. 5.

Fig. 6. Assessment of production of peroxynitrite in *E. coli*-challenged MSCs using dihydrorhodamine 123 probe.

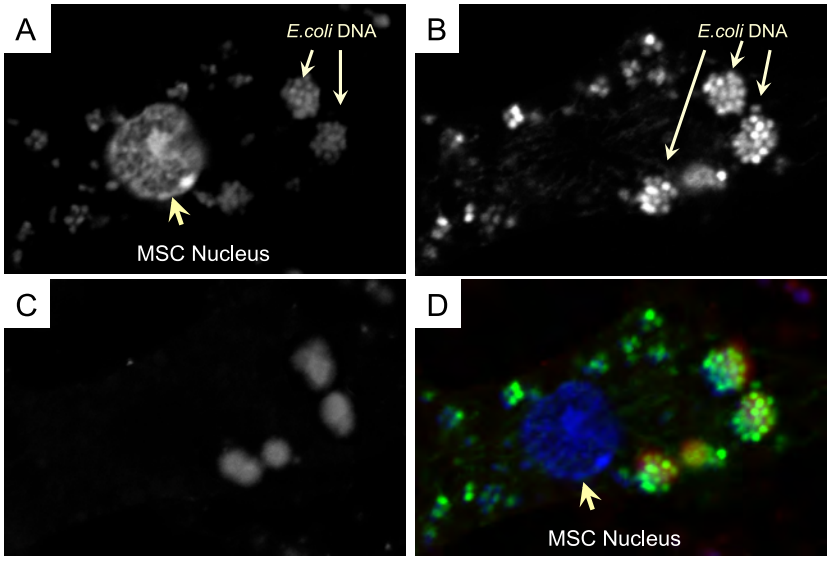

Panel A: Projection the nuclear DNA is indicated with yellow arrows (blue channel, counterstaining of nuclei with Hoechst 33342). Panel B: Projection of TUNEL-positive DNA (green channel). Panel C: Projection of tyrosine-phosphorylated caveolin-1 (red channel). Panel D: Overlay of the images presented in panels A, B, and C. TUNEL-positive bacterial nuclei appear in yellow as result of interference of blue and green. TUNEL – positive staining of bacterial DNA occurred in autolysosomes. Experimental conditions were the same as indicated in Fig. 5.

Fig. 7. Assessment of bacterial DNA damage in *E. coli*-challenged MSCs using terminal deoxynucleotidyl transferase dUTP nick-end labeling (TUNEL).

3.2 Stress-response of MSCs following challenge with *E. coli* bacteria

General stress responses are characterized by conserved signaling modules that are interconnected to the cellular adaptive mechanisms. It is proposed that stress induced by inflammatory factors, microorganisms, and oxidants triggers a cascade of responses attributed to specific sensitive transcriptional and post-transcriptional mechanisms mediating inflammation, antioxidant response, adaptation, and remodeling (36-42). The components of the oxidative stress response employ a battery of redox-sensitive thiol-containing molecules, such as glutathione (GSH), thioredoxin 1 (TRX1)/thioredoxin reductase, apurinic/apyrimidinic endonuclease/redox effector factor-1 (APE/Ref-1), and transcription factors (such as nuclear factor-kappa B (NF-κB) and nuclear factor (erythroid-derived 2)-like 2 (Nrf2). Overall, these effector proteins play a major role in maintaining the steady-state intracellular balance between pro-oxidant production, antioxidant capacity, and repair of oxidative damage (39, 43). While NF-κB and Nrf2 are normally sequestered in the cytoplasm bound to their native inhibitors, i.e., IκB and Keap-1 respectively, bacterial products, pro-inflammatory factors, and oxidative stress can stimulate their translocation to the nucleus (38, 41, 44). NF-κB and Nrf2 are known to regulate numerous genes that play a crucial role in the host response to sepsis (40, 45) and therefore, have relevance to the current study. Regulation of Nrf2 function is controlled by numerous factors among which Nrf2 conjugates with Keap-1.

Dissociation of the Nrf2/Keap-1 complex results from a modification of cysteine residues in Keap-1 through either their conjugation or oxidation (40, 43, 45).

Two major redox systems, the GSH and TRX1 systems, control intracellular thiol/disulfide redox environments. While the GSH/GSSG couple provides a major cellular redox buffer, TRXs serve a more specific function in regulating redox-sensitive proteins (46). These two redox systems function at different sites in the Nrf2 signaling pathway: first, the cytoplasmic dissociation of Nrf2 is primarily regulated by cytoplasmic GSH concentrations, and second, the nuclear reduction of Nrf2 cysteine 506 (required for Nrf2 binding of DNA) is primarily regulated by TRX1 (45). Redox dependence of DNA-binding activity of NF-κB has been broadly discussed (39, 47). DNA-binding activity of NF-κB can drastically increase in the presence of the reduced form of the redox factor-1 (Ref-1) redox-converted by TRX (39, 47). It should be noted that up-regulation of Nrf2 and NF-κB via autophagy-dependent mechanisms can also occur *via* lysosomal degradation of IκB and Keap-1, (48). Therefore, we do not exclude autophagy-dependent activation of these transcriptional factors in *E. coli*-treated cells. Taking into consideration all of the above, one would assume that a battery of stress-sensitive mechanisms mediated by survival transcription factors such as NF-κB, Nrf2, and FOXO3a are involved in adaptive response of MSCs challenged with *E. coli*.

Immunoblot analysis of stress-response proteins indicated that control MSCs had relatively high amounts of constitutively present NF-κB. Challenge of cells with *E. coli* resulted in prompt (within 1 h) increases in the nuclear fraction of NF-κB as determined with confocal immunofluorescence imaging (not shown). But, we did not observe a similar pattern when we assessed nuclear Nrf2. That could be due to an extremely low level of constitutive Nrf2 in the cells (Fig. 3). A drastic increase in the nuclear fraction of NF-κB occurred during the period of the observation, i.e., 24 h post-exposure (Fig. 8). This effect was accompanied

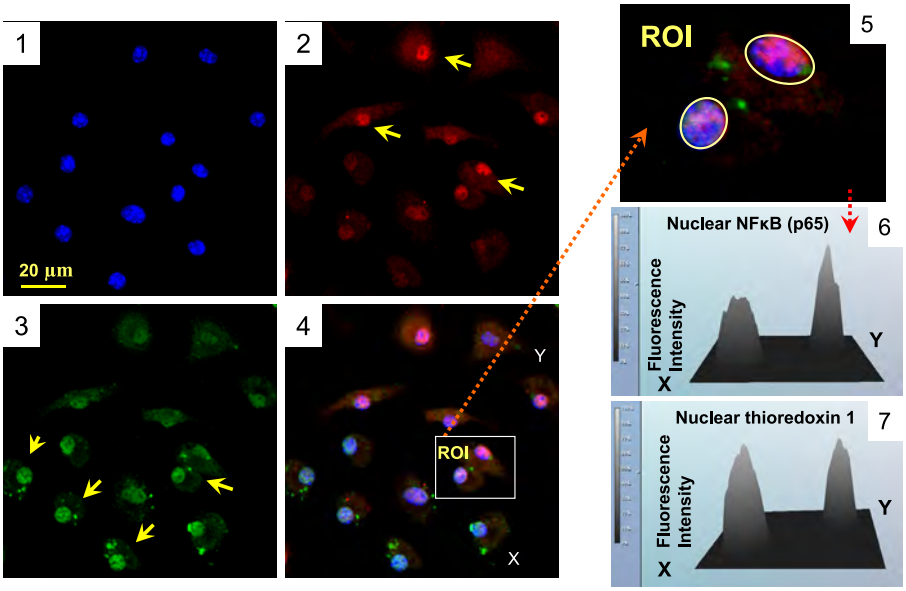

A

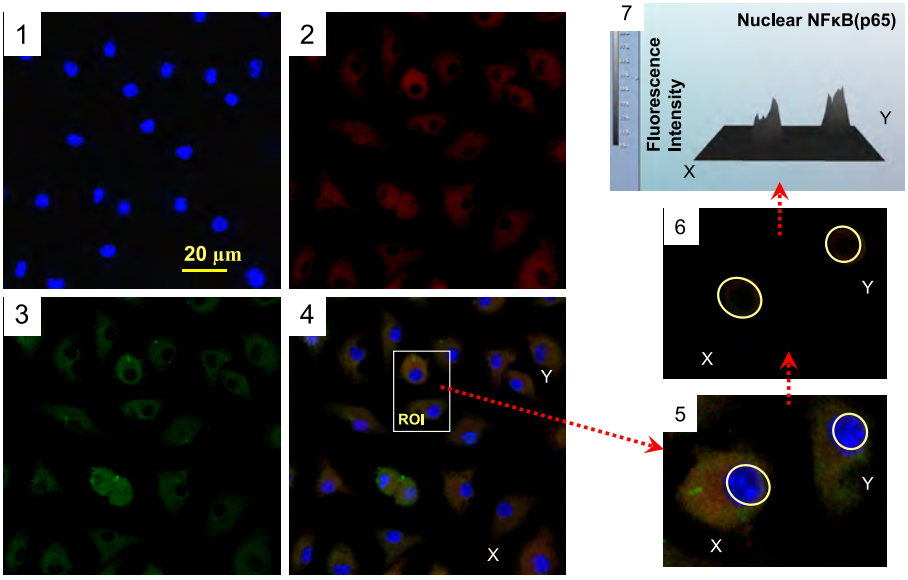

B

Panel 1: Projection of the nuclear DNA (blue channel, counterstaining of nuclei with Hoechst 33342). Panel 2: Projection of NFκB(p65) (red channel, nuclear localization is indicated with yellow arrows). Panel 3: Projection of thioredoxin 1 (green channel, nuclear localization is indicated with yellow arrows). Panel 4: Overlay of the images presented in panels 1, 2, and 3. Panels 5-7: analysis of nuclear fractions of NFκB(p65) and thioredoxin 1 in ROI indicated in panel 4. Experimental conditions were the same as indicated in Fig. 5.

Fig. 8. Assessment of nuclear fractions of NF-κB(p65) and thioredoxin 1 in MSCs challenged with *E. coli*. (A) Challenge with *E. coli*.; (B) Control.

by transactivation of NF-κB-dependent proinflammatory factors such as IL-1α, IL-1β, IL-6, and iNOS (Fig. 9). Interestingly, pre-incubation of the cells with pyrrolidine dithiocarbamate, an inhibitor of NF-κB translocation, resulted in development of pro-apoptotic alterations and loss of confluency in *E. coli*-treated MSCs (not shown). The response to *E. coli*–induced stress was also associated with increases in nuclear fractions of Ref-1 and TRX-1 (Figs. 8 and 10); these reducing agents appeared in close proximity with the nuclear NF-κB (Figs. 8 and 10). Moreover, the MSC stress-response at 24 h was characterized by significant expression of Nrf2 protein (Fig. 3) that accumulated in cell nuclei (Fig. 11). Based on these observations we concluded that the MSC response to challenge with *E. coli* activates complex molecular machinery designed to eliminate environmental microorganisms and increase adaptive capacity to stress. That conclusion contributes to a broad perspective on the role of stromal cells in the host innate defense and on the cell molecular mechanisms mediating resistance of cells to damage. Considering that the cell can

employ a battery of stress-response factors operating synchronously, we focused our attention on other cellular components that are crucial for cell survival, e.g., mitochondria, the caveolae vesicular system, and signaling cascades mediated by transcriptional factor FOXO3a.

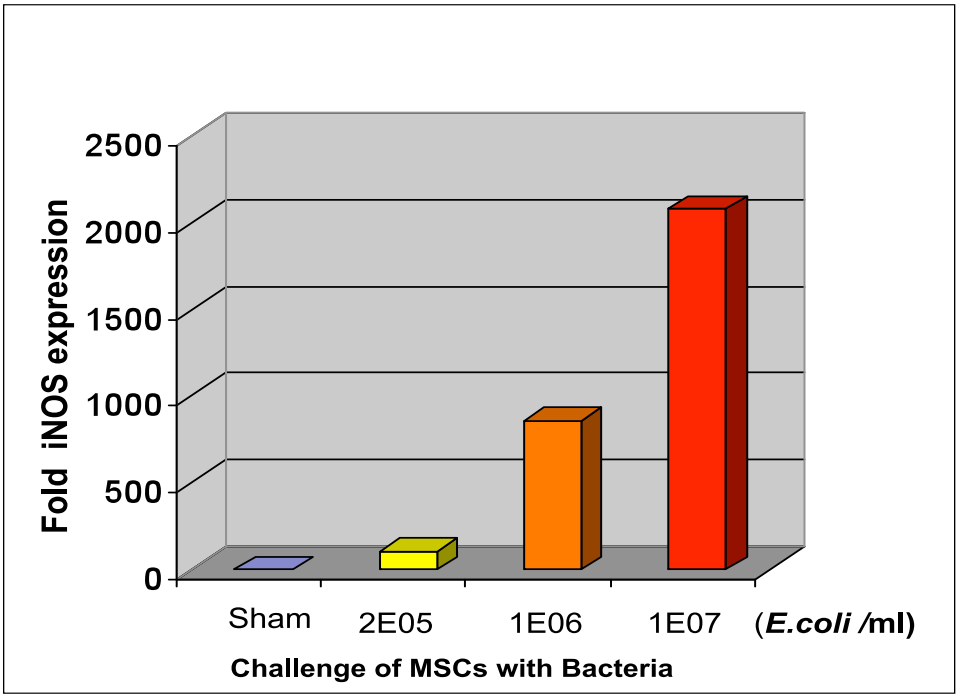

Fig. 9. qRT-PCR assessment of iNOS transactivation in MSCs challenged with *E. coli*. Conditions: MSCs were incubated with bacteria for 3 h in MesenCult Medium (without antibiotics). After 3 h the cells were harvested and lysed for extraction of RNA.

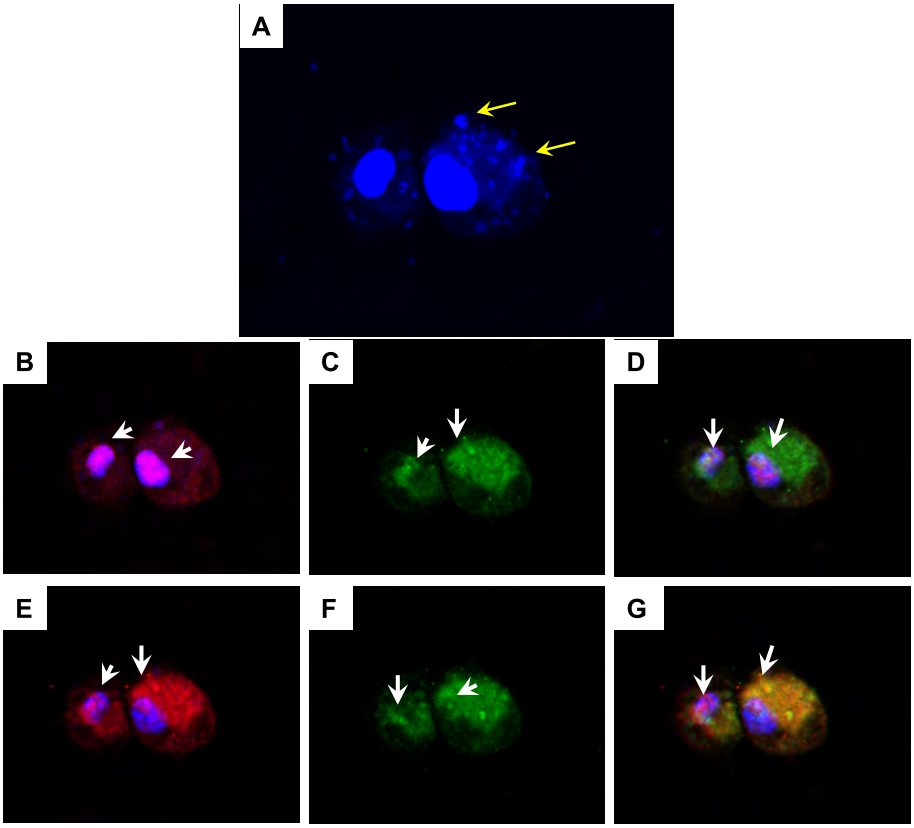

Panel A: Projection of the nuclear DNA (blue channel, high intensity; counterstaining of nuclei with Hoechst 33342). Bacterial nuclei are indicated with yellow arrow. Panel B: Projection of NFκB(p65) (red channel) and nuclear DNA (blue channel); nuclear co-localization of NFκB(p65) is indicated with white arrows. Panel C: Projection of Ref1 protein (green channel, nuclear localization is indicated with white arrows). Panel D: Overlay of the images presented in panels B and C. Nuclear co-localization of Ref1 and NFκB(p65) is indicated with white arrows. Panel E: Projection of Ref1 (red channel) and nuclear DNA (blue channel); nuclear co-localization of Ref1 is indicated with white arrows.
Panel F: Projection of thioredoxin 1 protein (green channel, nuclear localization is indicated with white arrows). Panel G: Overlay of the images presented in panels E and F. Nuclear co-localization of Ref1 and thioredoxin 1 is indicated with white arrows. Experimental conditions were the same as indicated in Fig. 5.

Fig. 10. Assessment of nuclear co-localization of NF-κB, thioredoxin 1, and Ref1 in MSCs challenged with *E. coli*.

FOXO3a, a member of a family of mammalian forkhead transcription factors of the class O, was recently proposed as mediator of diverse physiologic processes, including regulation of stress resistance and survival (49, 50). Thus, it is shown in our study that in response to oxidative stress, FOXO3a along with Nrf2 can promote cell survival by inducing the expression of antioxidant enzymes and factors involved in cell cycle withdrawal, such as the cyclin-dependent kinase inhibitor (CKI) p27 (50). We analyzed FOXO3a transcriptional factor in MSCs responding to *E. coli* challenge. Fig. 12 shows that the presence of *E. coli* increased FOXO3a protein in MSCs. The data suggest that, indeed, this FOXO3a transcriptional factor is also implicated in the stress-response to *E. coli* challenge.

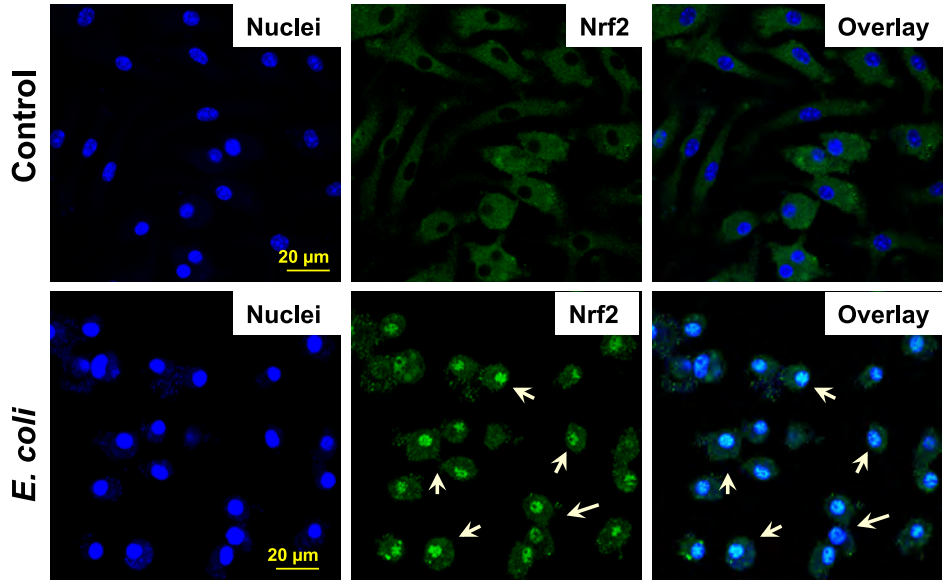

Fig. 11. Assessment of nuclear fractions of Nrf2 in MSCs challenged with *E. coli*. Counterstaining of nuclear DNA was with Hoechst 33342 (blue channel). Nrf2 staining is in green. Nrf2 localized in nuclei appears in turquoise/green color due to interference of "green" and "blue" (indicated with arrows). Experimental conditions were the same as indicated in Fig. 5.

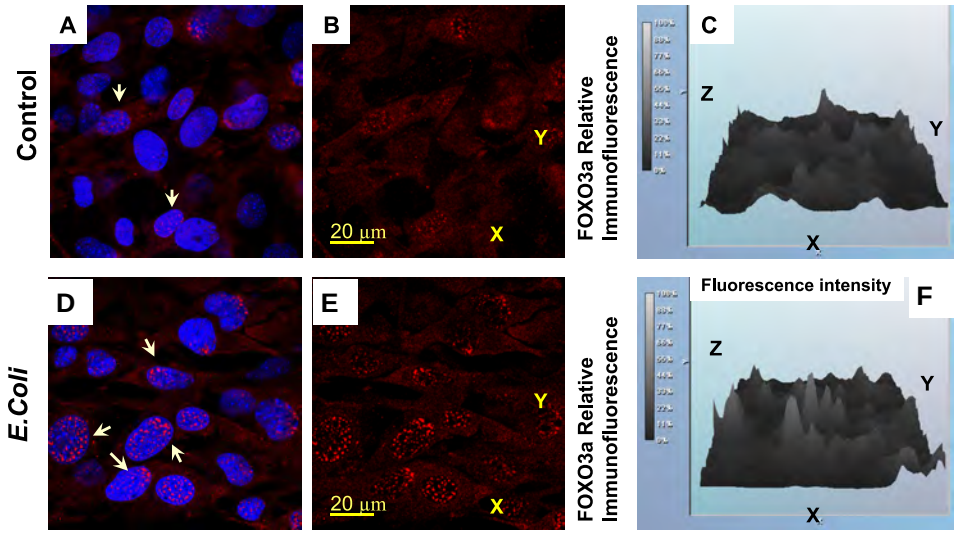

Control: Panel A-C. Challenged with *E. coli.*: Panels D-F.
Panels A and D: Projection of FOXO3a (red channel) and nuclear DNA (blue channel); nuclear localization of FOXO3a is indicated with white arrows. Panels B and E: Projection of FOXO3a protein (red channel only). Panel C and F: Relative intensity of the FOXO3a immunofluorescence shown in panels B and E, respectively. Experimental conditions were the same as indicated in Fig. 5.

Fig. 12. Immunofluorescence assessment of nuclear fraction of FOXO3a in MSCs challenged with *E. coli.*

4. Conclusion

Multipotent fibroblast-type mesenchymal cells are the essential components of the stroma, which supports tissue barriers and integrity (51). Disturbance in the stroma, composed of endothelial, fibroblastic and myofibroblastic cells as well as macrophages and other inflammatory cells - can be a critical step triggering bacterial translocation and sepsis - exacerbating a variety of injury types. This chapter aims to define whether MSCs can contribute to antibacterial innate defense mechanisms.

The antibacterial defense response of MSCs was characterized by extensive phagocytosis and inactivation of *E. coli* mediated by autolysosome mechanisms. *E. coli*-challenged MSCs showed increased transactivation of NF-κB, Nrf2, and FOXO3a stress-response transcriptional factors and associated expression of proinflammatory mediators. These observations were accompanied by a compensatory antioxidant response of MSCs mediated by nuclear translocation of Nrf2, Ref-1 and thioredoxin 1.

Taken together our data support the hypothesis that (i) MSCs contribute to the innate defense response to bacterial infection; (ii) the mechanism of MSC responses involves specific macroautophagy and nitroxidation mediated by iNOS; and (iii) MSCs are armed against self-injury by the mechanisms degrading phagocytized *E. coli.*

5. Acknowledgements

The authors thank HM1 Neil Agravante and Ms. Dilber Nurmemet for their technical support.

5.1 Grants

This work was supported by AFRRI Intramural RAB2CF (to JGK) and NIAID YI-AI-5045-04 (To JGK).

There are no ethical and financial conflicts in the presented work.

5.2 Disclaimer

The opinions or assertions contained herein are the authors' private views and are not to be construed as official or reflecting the views of the Uniformed Services University of the Health Sciences, AFRRI, the United States Department of Defense, or the National Institutes of Health.

6. References

[1] Turner HL, Turner JR. Good fences make good neighbors: Gastrointestinal mucosal structure. Gut Microbes. 2010; 1(1):22-9.

[2] Hooper LV, Macpherson AJ. Immune adaptations that maintain homeostasis with the intestinal microbiota. Nat Rev Immunol. 2010; 10(3):159-69.

[3] Wershil BK, Furuta GT. Gastrointestinal mucosal immunity. J Allergy Clin Immunol. 2008; 121(2 Suppl):S380-3.

[4] Vinh DC, Embil JM. Rapidly progressive soft tissue infections. Lancet Infect Dis. 2005; 5(8):501-13.

[5] Friedenstein A. Stromal-hematopoietic interrelationships: Maximov's ideas and modern models. Haematol Blood Transfus. 1989; 32:159-67.

[6] Sethe S, Scutt A, Stolzing A. Aging of mesenchymal stem cells. Ageing Res Rev. 2006; 5(1):91-116.

[7] Mezey E, Mayer B, Németh K. Unexpected roles for bone marrow stromal cells (or MSCs): a real promise for cellular, but not replacement, therapy. Oral Dis. 2010; 16(2):129-35.

[8] English K, French A, Wood KJ. Mesenchymal stromal cells: facilitators of successful transplantation? Cell Stem Cell. 2010; 7(4):431-42.

[9] McFarlin K, Gao X, Liu YB, Dulchavsky DS, Kwon D, Arbab AS, Bansal M, Li Y, Chopp M, Dulchavsky SA, Gautam SC. Bone marrow-derived mesenchymal stromal cells accelerate wound healing in the rat. Wound Repair Regen. 2006; 14(4):471-8.

[10] Tyndall A and Pistoia V. Mesenchymal stem cells combat sepsis. Nat Med. 2009; 15: 18 – 20.

[11] Krasnodembskaya A, Song Y, Fang X, Gupta N, Serikov V, Lee JW, Matthay MA. Antibacterial effect of human mesenchymal stem cells is mediated in part from secretion of the antimicrobial peptide LL-37. Stem Cells. 2010; 28(12):2229-38.

[12] Hall SE, Savill JS, Henson PM, Haslett C. Apoptotic neutrophils are phagocytosed by fibroblasts with participation of the fibroblast vitronectin receptor and involvement of a mannose/fucose-specific lectin. J Immunol. 1994; 153(7):3218-27.
[13] Levine B, Mizushima N, Virgin HW. Autophagy in immunity and inflammation. Nature. 2011; 469(7330):323-35.
[14] Yang Z, Klionsky DJ. Eaten alive: a history of macroautophagy. Nat Cell Biol. 2010; 12(9):814-22;
[15] Yano T, Kurata S. Intracellular recognition of pathogens and autophagy as an innate immune host defence. J Biochem. 2011; 150(2):143-9.
[16] Mizushima N, Levine B, Cuervo AM, Klionsky DJ. Nature. Autophagy fights disease through cellular self-digestion. 2008; 451:1069–75.
[17] Klionsky DJ. The Autophagy Connection. Dev Cell. Author manuscript; available in PMC 2011 July 20.
[18] Tooze SA, Yoshimori T. The origin of the autophagosomal membrane. Nat Cell Biol. 2010; 12(9):831-5.
[19] Weidberg H, Shvets E, Elazar Z. Biogenesis and cargo selectivity of autophagosomes. Annu Rev Biochem. 2011; 80:125-56.
[20] Eskelinen EL. New insights into the mechanisms of macroautophagy in mammalian cells. Int Rev Cell Mol Biol. 2008; 266:207-47.
[21] Eskelinen EL, Saftig P. Autophagy: a lysosomal degradation pathway with a central role in health and disease. Biochim Biophys Acta. 2009; 1793(4):664-73.
[22] Mizushima N, Levine B. Autophagy in mammalian development and differentiation. Nat Cell Biol. 2010; 12(9):823-30.
[23] Kabeya Y, Mizushima N, Yamamoto A, Oshitani-Okamoto S, Ohsumi Y, Yoshimori T. LC3, GABARAP and GATE16 localize to autophagosomal membrane depending on form-II formation. J Cell Sci. 2004; 117(Pt 13):2805-12.
[24] Behrends C, Sowa ME, Gygi SP, Harper JW. Network organization of the human autophagy system. Nature. 2010; 466(7302):68-76.
[25] Lipinski MM, Hoffman G, Ng A, Zhou W, Py BF, Hsu E, Liu X, Eisenberg J, Liu J, Blenis J, Xavier RJ, Yuan J. A genome-wide siRNA screen reveals multiple mTORC1 independent signaling pathways regulating autophagy under normal nutritional conditions. Dev Cell. 2010; 18(6):1041-52.
[26] Viiri J, Hyttinen JM, Ryhänen T, Rilla K, Paimela T, Kuusisto E, Siitonen A, Urtti A, Salminen A, Kaarniranta K. p62/sequestosome 1 as a regulator of proteasome inhibitor-induced autophagy in human retinal pigment epithelial cells. Mol Vis. 2010; 16:1399-414.
[27] Ryhänen T, Hyttinen JM, Kopitz J, Rilla K, Kuusisto E, Mannermaa E, Viiri J, Holmberg CI, Immonen I, Meri S, Parkkinen J, Eskelinen EL, Uusitalo H, Salminen A, Kaarniranta K. Crosstalk between Hsp70 molecular chaperone, lysosomes and proteasomes in autophagy-mediated proteolysis in human retinal pigment epithelial cells. J Cell Mol Med. 2009; 13(9B):3616-31.
[28] Behl C. BAG3 and friends: co-chaperones in selective autophagy during aging and disease. Autophagy. 2011; 7(7):795-8.

[29] Sridhar S, Botbol Y, Macian F, Cuervo AM. Autophagy and Disease: always two sides to a problem. J Pathol. 2011 Oct 12. doi: 10.1002/path.3025. [Epub ahead of print];

[30] Gorbunov NV, Garrison BR, Kiang JG. Response of crypt Paneth cells in the small intestine following total-body gamma-irradiation. Int J Immunopathol Pharmacol. 2010; 23(4):1111-23.

[31] Pfaffl MW. A new mathematical model for relative quantification in real-time RT-PCR. Nucleic Acids Res. 2001 29(9):2002-7.

[32] Nakagawa I, Amano A, Mizushima N, Yamamoto A, Yamaguxhi H, Kamimoto T, Nara A, Funao J, Nakata M, Tsuda K, Hamada S, Yoshimori T. Autophagy defends cells against invading Group A *Streptococcus*. Science. 2004; 306:1037-40.

[33] Yano T, Kurata S. Intracellular recognition of pathogens and autophagy as an innate immune host defence. J Biochem. 2011; 150(2):143-9.

[34] Xiao G. Autophagy and NF-kappaB: fight for fate. Cytokine Growth Factor Rev. 2007; 18(3-4):233-43.

[35] Ichimura Y, Komatsu M. Selective degradation of p62 by autophagy. Semin Immunopathol. 2010; 32(4):431-6.

[36] Kültz D. Molecular and evolutionary basis of the cellular stress response. Annu Rev Physiol. 2005; 67: 225-57.

[37] Burhans WC, Heintz NH. The cell cycle is a redox cycle: linking phase-specific targets to cell fate. Free Radic Biol Med. 2009; 47(9):1282-93.

[38] Sebban H, Courtois G. NF-kappaB and inflammation in genetic disease. Biochem Pharmacol. 2006; 72(9):1153-60.

[39] Janssen-Heininger YM, Mossman BT, Heintz NH, Forman HJ, Kalyanaraman B, Finkel T, Stamler JS, Rhee SG, van der Vliet A. Redox-based regulation of signal transduction: principles, pitfalls, and promises. Free Radic Biol Med. 2008; 45(1):1-17.

[40] Nguyen T, Nioi P, Pickett CB. The Nrf2-Antioxidant Response Element Signaling Pathway and Its Activation by Oxidative Stress J Biol Chem. 2009; 284(20):13291-5.

[41] Thimmulappa RK, Lee H, Rangasamy T, Reddy SP, Yamamoto M, Kensler TW, Biswal S. Nrf2 is a critical regulator of the innate immune response and survival during experimental sepsis. J Clin Invest. 2006; 116(4):984-95.

[42] Nivon M, Richet E, Codogno P, Arrigo AP, Kretz-Remy C. Autophagy activation by NFkappaB is essential for cell survival after heat shock. Autophagy. 2009; 5(6):766-83.

[43] Maher J, Yamamoto M. The rise of antioxidant signaling--the evolution and hormetic actions of Nrf2. Toxicol Appl Pharmacol. 2010; 244(1):4-15.

[44] Cronin JG, Turner ML, Goetze L, Bryant CE, Sheldon IM. Toll-Like Receptor 4 and MYD88-Dependent Signaling Mechanisms of the Innate Immune System Are Essential for the Response to Lipopolysaccharide by Epithelial and Stromal Cells of the Bovine Endometrium. Biol Reprod. 2011 Nov 2. [Epub ahead of print].

[45] Hansen JM, Watson WH, Jones DP. Compartmentation of Nrf-2 redox control: regulation of cytoplasmic activation by glutathione and DNA binding by thioredoxin-1. Toxicol Sci. 2004; 82(1):308-17.

[46] Jones DP. Methods Enzymol. 2002; 348:93-112. Redox potential of GSH/GSSG couple: assay and biological significance.

[47] Nishi T, Shimizu N, Hiramoto M, Sato I, Yamaguchi Y, Hasegawa M, Aizawa S, Tanaka H, Kataoka K, Watanabe H, Handa H. Spatial redox regulation of a critical cysteine residue of NF-kappa B in vivo. J Biol Chem. 2002; 277(46):44548-56.

[48] Weidberg H, Shvets E, Elazar Z. Biogenesis and cargo selectivity of autophagosomes. Annu Rev Biochem. 2011; 80:125-56.

[49] Miyamoto K, Araki KY, Naka K, Arai F, Takubo K, Yamazaki S, Matsuoka S, Miyamoto T, Ito K, Ohmura M, Chen C, Hosokawa K, Nakauchi H, Nakayama K, Nakayama KI, Harada M, Motoyama N, Suda T, Hirao A. Foxo3a is essential for maintenance of the hematopoietic stem cell pool. Cell Stem Cell. 2007; 1(1):101-12.

[50] Burhans WC, Heintz NH. The cell cycle is a redox cycle: linking phase-specific targets to cell fate. Free Radic Biol Med. 2009; 47(9):1282-93.

[51] Powell DW, Pinchuk IV, Saada JI, Chen X, Mifflin RC. Mesenchymal cells of the intestinal lamina propria. Annu Rev Physiol. 2011; 73:213-37.